Mechanics of Advanced Composite Structures

Journal homepage: https://macs.semnan.ac.ir/

Semnan University

ISSN: 2423-7043

Research Article

Patch Antennas with PDMS Substrate to Detect Tumors and their Data Transmission through ERPO-OFDM Modulation Technique in VLC

Karthikeyan Thavittupalayam Angappan[a]*, Nesasudha Moses [a], Anitha Vijayalakshmi [b]

[a] *Department of ECE, Karunya Institute of Technology and Sciences, Coimbatore, 641114, India*

[b] *Department of ECE, Saveetha School of Engineering, Chennai, 602105, India*

ARTICLE INFO

Article history:

Received: 2023-03-22
Revised: 2023-05-12
Accepted: 2023-10-19

Keywords:

Patch Antenna; Visible Light Communication; Health care; Tumor; LEDs.

ABSTRACT

A Patch antenna is a kind of antenna with a low profile, which can be fixed on a surface. It communicates and gets electromagnetic waves inferred way. The boundaries of the antenna incorporate radiation design, gain, impedance, and frequency. Polydimethylsiloxane (PDMS) is utilized as a substrate in patch antennas. The existence of a tumor can be effectively recognized by the current density of the phantom. The difference in the current density value of phantom without tumor and with tumor shows the presence of the tumor. The first four antenna designs show a huge contrast in current density, the leftover two designs have little distinction of current density worth of phantoms. Six unique constructions of microstrip antenna are intended for skin tumor detection. In these six designs, the model for skin cancer recognition utilizing truncated corner, the working frequency is 2.492 GHz and S11 is –38 dB. The current density of the design relies on phantom characteristics. The acquired current density value of phantom without the growth of the tumor, with tumor, and with dangerous growth of the malignant tumor is (171.562, 193.381, and 204.199) A/m^2 and the Specific Absorption Rate (SAR) value is (1.14049, 1.27013 and 1.26088) W/Kg respectively. Visible Light Communication (VLC) system using Orthogonal Frequency Division Multiplexing (OFDM) supports high-speed transmission. The effectively-identified tumor can be communicated through gadgets using Enhanced Reverse Polarity Optical OFDM (ERPO-OFDM) technique. It's a multicarrier modulation that supports information transmission through Light Emitting Diodes (LEDs).

1. Introduction

Lately, wearable electronics and related innovations have more demand [1]. The fundamental benefits are scaling down of remote, small size, great battery choice, and less force utilization. The wearable antenna is only the antenna that capacities while worn; a large portion of biomedical applications favor this kind of antenna [2]. For instance smart watches, smart glasses, and so forth there are numerous common difficulties while planning antenna and it makes the plan interaction troublesome. The wearable gadget shouldn't influence the human body as it assimilates electromagnetic waves and upsets.

* **Corresponding author.**
E-mail address: karthikeyant20@karunya.edu.in

Cite this article as:
Mohammadi, A., Mahdi-Nia, M., 2024. Title of article. *Mechanics of Advanced Composite Structures*, 11(2), pp. 1402-1425
https://doi.org/10.22075/MACS.2023.39315.2050

The consequence of the wearable antenna might change when it is set close to the human body [3]. And the wearable gadget ought to be small in size which is additionally a test while planning the antenna. Antennas are planned dependent on the prerequisites like bandwidth, efficiency, size, application, and polarization. As of late stretchable electronics are better known because of their extending capacity [4]. The properties of electric substrates are essential to stretchable gadgets [5–7]. In the majority of the stretchable receiving wires, PDMS is utilized as substrate. It has many benefits including good chemical properties, thermal stability, transparency, and biological compatibility.

In [8] For this application, a 1.6 mm thick dielectric substrate with a dielectric constant of 4.7 made of denim material is presented. For the best antenna output, this wearable antenna, designed for 2.45 GHz applications, uses the conducting type's co-axial feeding technology. This antenna is simulated using CST software, and the simulation output is compared to previously recorded parameters such as directivity (D), gain in dB, return loss (S11), and VSWR.

The 2.4 GHz single band inset-fed rectangular microstrip patch antenna design is presented in this paper and the antenna is simulated in CST [9]. The substrate dielectric constant, the loss tangent of 0.019, and the resonant frequency of 2.45 GHz are the three main design parameters that are specifically mentioned. The 3-D gain plot, return loss, voltage standing wave ratio (VSWR), directivity for the H-plane (φ = 90°), directivity for the E-plane (φ = 0°), and other antenna performance metrics are acquired from the simulation. With a bandwidth of 68.3 MHz, the simulation results indicate a minimum return loss of -26.394 dB. While many antennas have great gain and precision for the early detection of breast cancer, the flexible microstrip patch antenna has a higher efficiency than other antennas

An overview of PDMS's characteristics and a few of its widely utilized treatments are provided in this review to ensure that it is appropriate for those fields [10]. Applications are also reviewed, including medical implants, cardiovascular flow replication, and microchips in the biomedical industry. Suitable optical, electrical, and mechanical qualities make polydimethylsiloxane (PDMS) a suitable elastomer for a variety of technical applications. PDMS is frequently utilized in the biomedical field because of its biocompatibility. The soft-lithography technology, which was developed to enable the quick prototyping of micro and nanostructures using elastomeric materials—most notably PDMS—has also become more widely used. Applications are also reviewed, including medical implants, cardiovascular flow replication, and microchips in the biomedical industry.

The skin is the biggest organ of the body with a complete space of around 20 square feet. The skin shields us from organisms and the components assist standard with bodying temperature and license the vibe of touch, hotness, and cold. The epidermis, Dermis, and Hypodermis are three layers of skin. The furthest layer of skin that gives water-confirmation obstructions is the epidermis, the layer that contains tissue, hair follicles, and sweat glands is the dermis, and the layer that is comprised of fat and connective tissue is the hypodermis. Dermatology is the part of science that manages skin conditions. Relative permittivity will be the permittivity of a given material compared with that of the permittivity of a vacuum. PDMS substrate is picked by thinking about the properties of substrate that are with Epsilon 2.8 and Tangent delta el 0.02 [11]. The boundaries like frequency, return loss, VSWR, gain, and bandwidth are determined and looked at.

The collected information about the tumor can be transmitted through the OFDM method, which supports high-speed data transmission. Several carrier frequencies are used to encrypt the digital data [12] in OFDM. High-order Multilevel Quadrature Amplitude Modulation (M-QAM) symbols on orthogonal subcarriers enhance data rate in optical wireless systems [13].

Parallel transmission of data in OFDM supports a high data rate. The bipolar signal can be converted into a unipolar signal in an optical system using Direct Current Biased OFDM (DCO-OFDM) and Asymmetrically Clipped Optical-OFDM (ACO-OFDM), which are the general schemes used to do the conversion. The Direct Current (DC) bias is added to the time domain signal [14] to produce the DCO-OFDM signal and negative excursions are completely clipped off [15] to create the ACO-OFDM signal and its non-negative. Odd indexed subcarriers are assigned with modulated data and the even indexed subcarriers are set to zero in the ACO-OFDM technique [16]. The high-rate OFDM signal is combined with the slow-rate PWM signal in RPO-OFDM, which subsidizes the overall illumination of the LEDs [17]. In ERPO-OFDM, the LEDs are driven by the combination of RPO-OFDM data signal with DSM signal [1] and avoid the problem of flickering.

A simulation and design of a U-shaped slot antenna are shown in [18], along with an investigation of the antenna's performance with several flexible substrates. The RMSA is built using additional materials such as polyamide, polyethylene, PDMS, Teflon, RT Duroid, and

epoxy to manage the 2.4–2.6 GHz operating frequency. The characteristics of the antenna, including its cost, gain, radiation pattern, bandwidth, and reflection coefficient, are investigated by keeping each substrate at the same height. It has been established that the recommended antenna whose substrate material is PDMS is suitable for weight and health-tracking systems.

In this work [19] the impact of microstrip antenna array bending on breast tumor detection is examined in this paper. Antenna arrays with resonance frequencies of 2.4 GHz and return losses of less than -35 dB were built. The designed antenna is simulated and analyzed using CST software. The potential of this antenna is highlighted, and its bending effect and tumor-sensing ability are investigated. Based on its performance, this antenna seems to be a suitable option for breast tumor detection.

A patch antenna operating at 2.45 GHz was considered a potential breast tumor detection tool [20]. Realizing an effective and low-reflection antenna array is the ultimate goal, and it will require further investigation into antenna designs as well as tumor and phantom characteristics as a function of frequency. Consequently, an earlier detection of malignant cells in a woman's breast is possible with the use of this recommended technique.

Tumor detection has been the subject of numerous investigations, however flexible materials with low dielectric constant and loss tangent that are employed as substrate in WBAN applications are not studied well. The materials and their dielectric constant can maximize antenna size and functions are limited by this research gap. Thus, the purpose of this work is to investigate how a flexible substrate that is water resistant, optically transparent, and has good thermal stability might be used for WBAN applications to detect tumors.

The following highlights the importance of this work:

- Six distinct 2.45 GHz PDMS-based antennas are developed, and their respective performances are evaluated.
- Six distinct PDMS-based antennas are evaluated for performance on top of a stacked phantom consisting of two layers and a tumor in CST.
- When the antenna is mounted on the stack-layered phantom, its specific absorption rate is tested, and it is less than 1.6 W/kg.
- It has been determined that differences in antenna field overlays between phantoms with and without tumors can be utilized to identify tumor presence in biological fields.

This article is divided into four sections. Section I is the Introduction. A description of the microstrip antenna with WMBAN is given in Section II. In Section III, the results and discussions are presented. Section IV contains the Conclusions.

2. Microstrip Antennas with WMBAN

The wireless body area network is a sub-part of a wireless sensor network. A wireless body area network is additionally named a Wireless Body Area Network (WBAN), or Wireless Medical Body Area Network (WMBAN). Essentially it is a wireless network that is stabilized around the human body, to screen medical conditions. There are various gadgets utilized in WBAN such as medical sensors, Personal Digital Assistance (PDA), tablets, and so on as shown in Fig. 1. The WBAN has various applications, including temperature, blood pressure, sugar level, motion detection, and sensor individuals checking, and screen of warriors in war and space explorers in space.

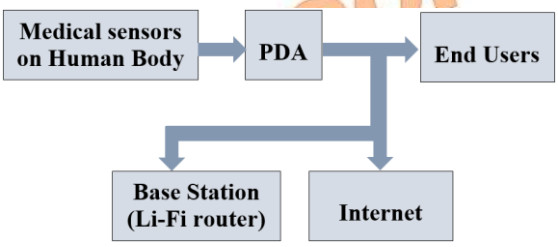

Fig. 1. Typical WBAN architecture

Microstrip patch antennas are likewise called patch antennae or microstrip antennas. Because of its lower weight and minimal expense, it is better-known features of being light, small, and planar structure microstrip antenna ought to have the advantage of being easy for wireless sensor applications [21]. A little piece of contacting material is patched and placed on the top side of the substrate and the ground comes on the bottom side of the substrate [22].On account of the size, weight, cost, and performance simplicity of establishment it has numerous applications. There are various states of microstrip patch components, they are square, rectangular, dipole, circular, elliptical, triangular, circle sector, circular, and ring-shaped. There are four feeding mechanisms in microstrip patch antenna they are microstrip line, aperture coupling and proximity coupling, and coaxial probe [23]. The restriction of the microstrip patch antenna is limited recurrence bandwidth and it very well may be over-stopped by expanding the thickness of the patch and adding responsive parts to diminish VSWR [24]. The central boundaries of the antenna are gain,

efficiency, bandwidth, polarization, directivity, radiation pattern, and input impedance.

2.1. Antenna Design

Six different shapes of the antenna are designed. This simple square antenna as shown in Fig. 4(a) is the first base model of all designs. There are three layers ground, substrate, and patch. PDMS is used as the substrate, one side of the substrate is attached to the ground and the other side is patch. Co-axial feed is used as antenna feed. The following table 1 shows the measurement used to design the antenna and it is mentioned in Fig. 2. In this design, the co-axial feed is shown in Fig. 3, and the co-axial feed has the following measurements as shown in Table 2.

Table 1. Dimensions of the antenna

Parameters	Dimensions (mm)
Ground and Substrate Width	40
Length of the antenna	40
The thickness of the Ground and Patch	0.035
The thickness of the substrate	1
Width and length of patch	35.5

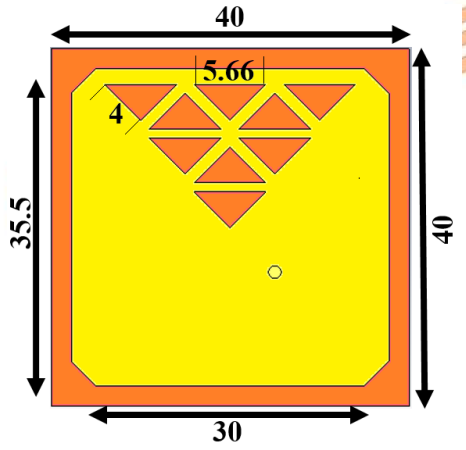

Fig. 2. Measurements of the patch antenna

Table 2. Measurements of the coaxial feed

Type	Material	Inner radius	Outer radius
Feed	PEC	0.0	0.7
Coax	PEC	0.7	1.59
Outer coax	PEC	1.59	1.6

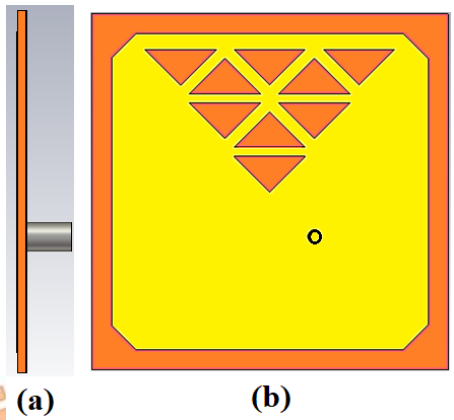

Fig. 3. Side view and back view of the coaxial feed

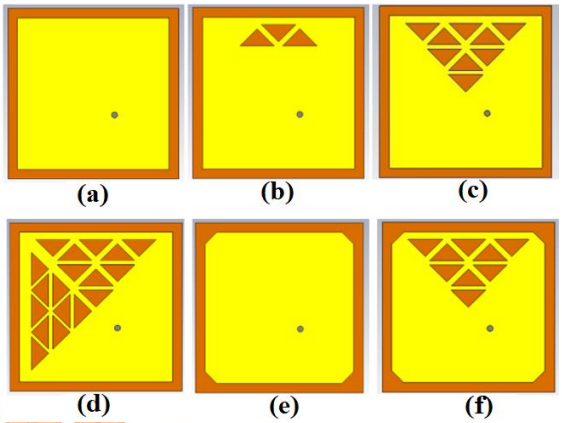

Fig. 4. (a) Simple square (b) Square with 3 triangle slots (c) Square with 9 triangle slots (d) Square with 18 triangle slots (e) Truncated corner (f) Truncated corner with 9 triangular slots

2.2. Phantom Design

Skin, fat, and tumor are the three layers of the phantom. The dimensions of the phantom from Table 3 and material properties as shown in Table 4 created for the skin phantom.

Table 3. Measurements of skin phantom

Layers	Length	Breadth	Thickness
Skin	60	60	20
Fat	56	56	10
Tumor	10	10	20

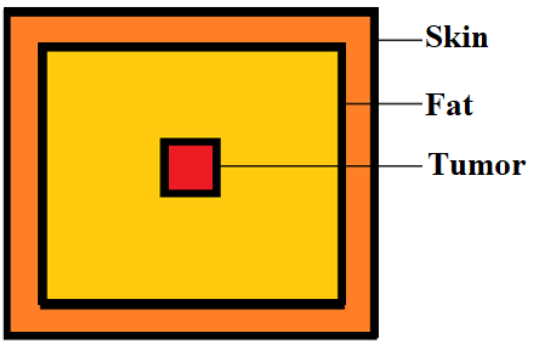

Fig. 5. Phantom structures

Table 4. Material properties of skin phantom

	Permittivity (F/m)	Density (Kg/m^3)	Electrical Conductance [S/m]
Skin	33.083	1100	5.9391
Fat	4.753	910	0.45075
Tumor	50.821	1041	4
Malignant tumor	67.000	1041	4

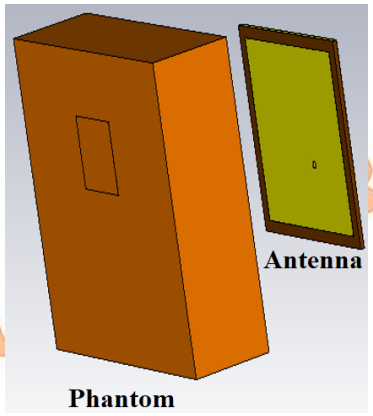

Fig. 6. Patch antenna on top of skin phantom

By using these parameter values [25], skin phantom in CST is designed as shown in Fig. . 5. The distance between the skin and the patch is maintained at 10mm [26]. The patch antenna is placed on top of the skin phantom as depicted in Fig. 6.

3. Results and Discussion

There are six different designs they are Simple Square, 3 triangles, 9 triangles, 18 triangles, truncated corner, truncated corner with 9 triangles. Every design had three modes that is each design is simulated with the skin phantom.

Table 5 shows the comparison of results with six different patch antennae. That skin phantom might be without a tumor, with a tumor, and with a malignant tumor. A total of 18 modes of design and their results are compared in Table 5 and Table 6. These total 18 models of designs are simulated separately and their corresponding results S11, frequency, bandwidth, VSWR, current density, E-Field, H-field, directivity, gain, and SAR values are calculated and tabulated.

From Table 5 and Table 6, it is observed that the return loss is greater in Simple Square and truncated corners. All the operating frequency of designs is between 2.2 to 2.5 GHz. The rate at which energy is absorbed by the human body per unit mass when subjected to an electromagnetic field with a radio frequency (RF) is known as the specific absorption rate, or SAR. These six antenna models are positioned on skin phantoms that are benign, cancerous, or have no tumor at all. According to the Federal Communication Commission (FCC) norm, the SAR values obtained for each of the six antenna models are less than 1.6W/Kg. Furthermore, in comparison to other antennas, the 18 triangular antenna model has an extremely low value of 0.78 W/kg. In this paper, the presence of a tumor is detected using the current density values [27].

The difference in current density value without tumor and with tumor is used to detect the tumor. So in these six designs of a patch antenna, truncated corner and truncated corner with 9 triangle slots have much difference in current density value. The truncated corner patch antenna design has having good return loss value and better current density difference value. Thus the truncated corner design is good when compared to all the remaining designs. The current density worth of the truncated corner design shows higher contrast when compared with all designs.

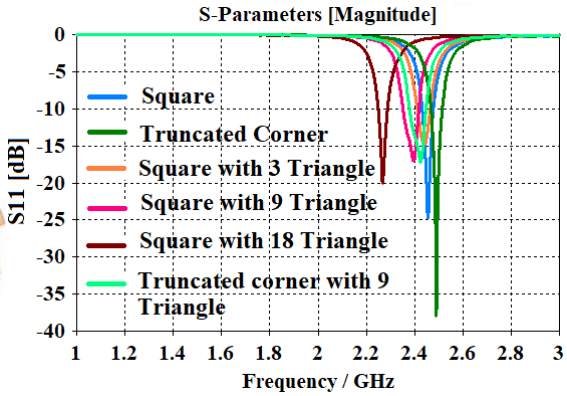

Fig. 7. Operating frequency

The return loss of the six model antenna is plotted and depicted in Fig. 7. While there may be a small variation in frequency, all antenna models are found to work at 2.45 GHz, with the antenna's entire bandwidth still covering this frequency range. The truncated corner antenna model is seen to operate at the appropriate frequency with good S11 and bandwidth, as shown in Fig. 7. The resonant frequency of the PDMS antenna with phantom and without phantom is plotted separately [28] and the resonant frequency varies with different designs. The return loss S11 boundary expresses the quantity of power reflected from the antenna. All the antenna design shows the variation in current density. Some design shows less distinction of significant worth and a few show more contrast of current density with and without tumor.

Table 5. Comparison of results with first three design patch antennae

	Simple Square			3 Triangle			9 Triangle		
	Without Tumor	With Tumor	With Malignant Tumor	Without Tumor	With Tumor	With Malignant Tumor	Without Tumor	With Tumor	With Malignant Tumor
S 1,1	-43.58	-42.06	-42.3741	-16.04	-16.12	-16.0976	-16.97	-17.05	-17.0421
Frequency (GHz)	2.462	2.462	2.462	2.448	2.448	2.448	2.396	2.396	2.396
Bandwidth (MHz)	44.5	45.3	44.8	57.1	57.1	57.1	65.6	65.4	65.8
VSWR	1.0133	1.0159	1.01533	1.3744	1.3706	1.37169	1.3304	1.3267	1.32713
Current Density (A/m^2)	163.3	187.9	199,057	156.02	158.91	172.676	156.27	158.06	164.578
E-Field (V/m)	30399	30393	30380	27366	27435	27419.1	27911	27979	27976.3
H-Field (A/m)	100.02	100.25	100.047	129.32	129.66	129.607	184.06	184.32	137.106
Directivity	2.875	2.844	2.856	2.873	2.841	2.853	2.829	2.8	2.807
Gain	0.4455	0.4395	0.4431	0.4407	0.4345	0.438	0.397	0.3916	0.3939
SAR 1g (W/Kg)	1.0889	1.09	1.11338	1.1109	1.1065	1.11032	1.0652	1.0627	1.0658

Table 6. Comparison of results with next three design patch antennae

	18 Triangle			Truncated Corner			Truncated With 9 Triangle		
	Without Tumor	With Tumor	With Malignant Tumor	Without Tumor	With Tumor	With Malignant Tumor	Without Tumor	With Tumor	With Malignant Tumor
S 1,1	-20.01	-20.02	-20.0496	-38.01	-39.83	-41.4847	-17.23	-17.27	-17.2624
Frequency (GHz)	2.268	2.268	2.268	2.492	2.492	2.492	2.424	2.426	2.426
Bandwidth (MHz)	38	38	38	45	46	46	67	67	67
VSWR	1.2218	1.2216	1.22082	1.0255	1.0206	1.017	1.3189	1.3172	1.31763
Current Density (A/m^2)	187.57	187.75	187.679	171.56	193.38	204.199	160.6	171.31	171.292
E-Field (V/m)	37747	37771	37756.6	29549	41151	41130.1	36936	39030	39027.5
H-Field (A/m)	214.59	214.48	214.396	98.122	97.619	97.3661	182.86	184.03	183.903
Directivity	2.714	2.687	2.688	2.815	2.788	2.802	2.774	2.747	2.755
Gain	0.3031	0.2987	0.2993	0.463	0.4584	0.4624	0.4165	0.4112	0.4138
SAR 1g (W/Kg)	0.7874	0.7947	0.79146	1.1405	1.2701	1.27088	1.1202	1.1245	1.12771

Figure 8 depicted that the VSWR of truncated patch antennas is 1.02 and also the VSWR of each of the six designs is less than 2. It shows the use of this antenna for wireless applications. A VSWR of less than two is regarded as slightly acceptable in WBAN applications, as can be seen in Fig. 8. As a result, the proposed antenna transmits radio frequency power effectively.

The Voltage Standing Wave Ratio is the extent of how much power is communicated starting from the source to the store. It extends between generally outrageous to least voltage in a standing wave. The specific absorption rate is measured in CST, which shows that for all antenna models, the SAR ought to be less than 1.6W/Kg. The truncated patch antenna with 1.14 W/Kg of SAR when it is mounted on the stack-

layered phantom, is shown in Fig. 9. According to the FCC, the antenna's standard SAR value indicates that it is suitable for use with wireless body area networks (WBANs). Therefore, from Fig. 9, this proposed antenna can be used for the human body to identify malignancies. When a PDA or other remote device is sent, the amount of RF power that remains in the human body is known as SAR. During SAR consistency testing the best SAR value is evaluated in Watts/kilogram.

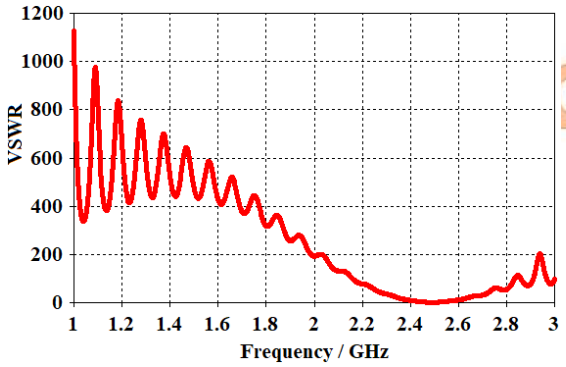

Fig. 8. VSWR

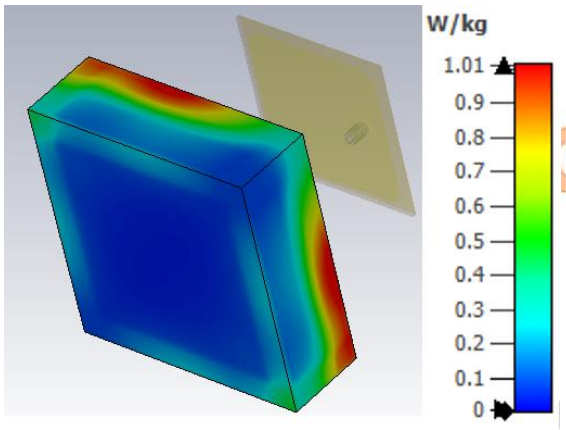

Fig. 9. Specific Absorption Rate

3.1. Fabrication and Measurements

Figure 10 shows the schematic diagram that was used to explain the proposed antenna's technique. When creating and modeling an antenna, choosing the right frequency and material is essential. Once the antenna is designed for the intended frequency, it is mounted atop the phantom. The chosen materials are then used to fabricate the antenna. All Copper foil is used as the patch and ground, while flexible PDMS is used as the substrate for the built and simulated antenna. The substrate is 1 mm thick, and to create PDMS, Sylgard base elastomer and curing agent are mixed in a 10:1 ratio before the mixture is put in a vacuum desiccator to quickly remove moisture and air. Pouring the solution into a glass mold with a thickness of 1 mm allows for the necessary substrate material thickness, and the mold is then placed in a 500 C microwave oven to cure. Following the settling phase, the PDMS is removed from the mold, and the workflow for synthesizing the PDMS is depicted in Fig. 11.

After following substrate preparation, the copper foil is sized and cut to fit the substrate's dimensions. As depicted in Fig. 12, the top side of the substrate is joined with a copper patch, and the bottom side is joined with copper ground. Using the same axis as the intended antenna, the female SMA connection is soldered as a coaxial feed after being placed into the antenna's three layers. The constructed antenna's measuring configuration using a ruler is shown in Fig. 12. The length and width of the fabricated antenna are identical to those of the simulated antenna.

The fabricated antenna is measured in the anechoic chamber by attaching it to a connector of the anechoic chamber as depicted in Fig. 13, and the Vector Network Analyzer is used to analyze the reflection coefficient. The Anechoic chambers are spaces created to limit interference from external spurious energy sources and absorb electromagnetic radiation reflections. Because they are not reflective, these spaces are referred to as anechoic chambers. Anechoic chambers are used to measure the tested antenna gain, pattern features, and overall performance.

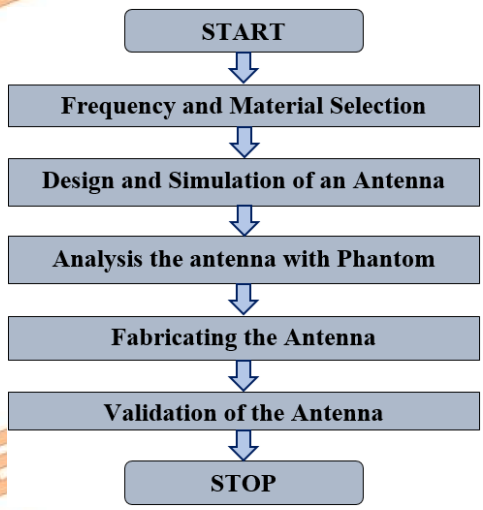

Fig. 10. Schematic diagram for the methodology of the proposed antenna

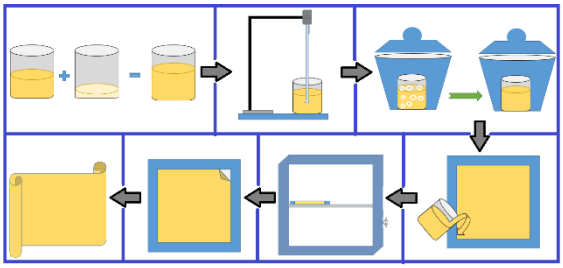

Fig. 11. Schematic diagram for synthesizing of PDMS for fabrication of the antenna

The purpose of the anechoic chamber wall's construction was to obstruct external signals that could affect the precision of the measurement. Moreover, it stops test signals from leaving the anechoic chamber, which could interfere with other instruments and be hazardous to health. Radar-absorbing material (RAM) is used in anechoic chambers in a configuration and arrangement designed to produce a quiet space and absorb radio frequency signals within the necessary frequency range. With the aid of VNA N9915A, Figure 14 depicts the observed antenna's reflection coefficient when the antenna is put within the anechoic chamber. When compared to the simulated antenna, there is a slight variation in S11 (2.54 GHz with S11 of -33.94 dB) values. This variation can be attributed to fabrication processes such as soldering and bonding copper foil to the substrate. In addition to the discrepancy between the fabricated and simulated antennas, the antenna's total bandwidth is still covering 2.4 GHz. Thus from Fig. 14, the fabricated antenna is hence appropriate for WBAN applications.

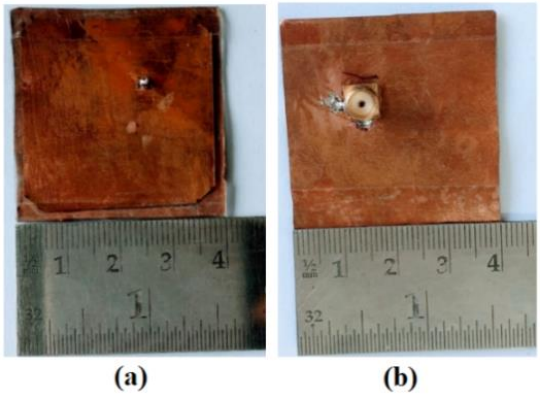

Fig. 12. Top and bottom view of the fabricated antenna

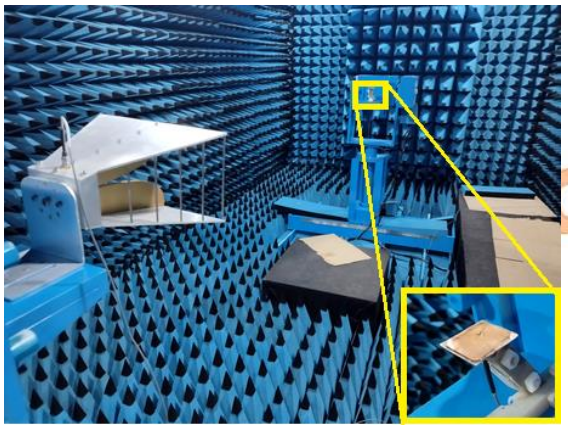

Fig. 13. Anechoic Chamber measurement setup

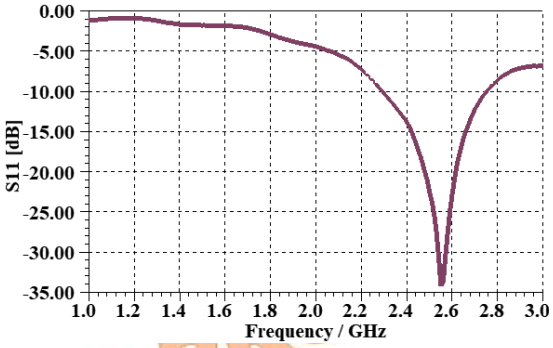

Fig. 14. Measured reflection coefficient

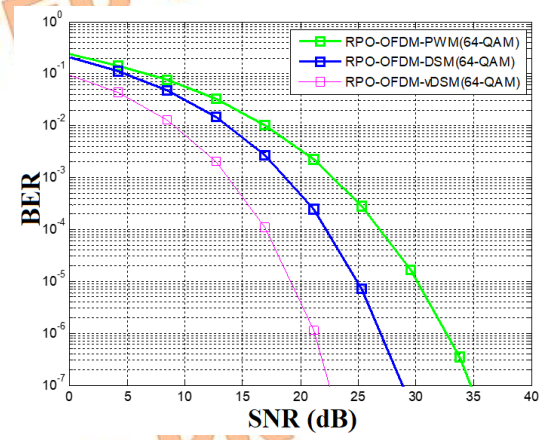

Fig. 15. BER versus SNR

The sensed information about the tumor is modulated using the ERPO-OFDM method and transmitted using VLC. The noted parameter while transmitting data about the tumor is the Bit Error Rate (BER). BER performance of conventional RPO-OFDM compared with ERPO-OFDM using 64-QAM is shown in Fig.15 [15]. The simulation output shows better BER performance of ERPO-OFDM when compared with traditional ones. The single OFDM symbol duration is 4μs and for 64-QAM the number of subcarriers is 48. The modulation technique ERPO-OFDM outperforms conventional OFDM. With the increase in constellation size, the BER increases.

Table 7 illustrates the way this study is compared to other related efforts. It provides an overview of all reported antenna substrates, frequency, size, application, Phantom structure, and SAR. The reported approach creates a variety of phantom models, including cube, semi-sphere, cylindrical, and imitating solutions. An artificial breast model in the shape of a semi-sphere is created in the proposed antenna configuration for tumor detection. There is also mention of the SAR analysis using these phantoms and its applications. Analysis reveals that, in comparison to alternative antenna designs, the proposed antenna's measurement is compact and modest.

Table 7. Comparison of reported work in the literature

Ref. No	Dimension	Substrate	Frequency	Application	Phantom Structure	SAR
[29]	60×60×2.4	PDMS	2.45 GHz	Implantable Bioelectronics	Cube	Tested
[19]	206×100×0.508	RO-4003C	2.45 GHz	Breast tumor Detection	Semi Sphere	-
[30]	80×70×3.2	PF4-Foam	2.45 and 5 GHz	WBAN	Cube	Tested
[31]	70×60×1.6	Cotton	1.6 to 11.2 GHz	Breast Cancer	Semi Sphere	-
[32]	70×25×2	Felt	2.45 GHz	BAN	Cylinder	-
[33]	100×20×9.24	Kapton	2.45 GHz	Radiation Dosimeter	Mimicking Solution	-
[34]	80×40×0.8	FR4	2.45 GHz	Breast Cancer	Cylindrical	Tested
This Paper	40×40×1	PDMS	2.45 GHz	Breast Tumor	Cube	Tested

4. Conclusion

Six different patch antennas with PDMS substrate are designed using CST. From the simulation, it is observed that the presence of a tumor can be easily detected from the current density value of antennas placed on a phantom that has a tumor and no tumor. All the antenna design shows the variation in current density. Some design shows less difference in value and some show more difference in current density as a tumor and no tumor. The current density value of the truncated corner design shows a higher difference when compared to all designs. The obtained Current density of the proposed antenna of the phantom having no tumor is 171(A/m^2), for the phantom having a tumor is 193 (A/m^2), and for the phantom having a malignant tumor is 204.199 (A/m^2). Similarly, the E-field and H-field also show the difference between a phantom having a tumor and having no tumor. The E-field values of the proposed antenna having no tumor is 29549(V/m), for phantom having a tumor 41151 (V/m), and for phantom having a malignant tumor is 41130 (V/m). The Magnetic field values of the proposed antenna having no tumor is 98.122 (A/m), for phantom having a tumor 97.619 (A/m), and for phantom having a malignant tumor is 97.3661 (A/m). All different parameters such as VSWR, gain, and return loss, are calculated. The SAR value is calculated for all designs and it comes to fewer than 1.6 W/Kg over 1gm of tissue. Thus the presence of a tumor can be easily detected. The observed information regarding the tumor is transmitted through the ERPO-OFDM technique in VLC. It offers better BER than conventional OFDM while transmitting the tumor information using LEDs.

Funding Statement

The submitted work did not receive any support from any organization.

Conflicts of Interest

The author declares that there are no conflicts of interest regarding the publication of this article.

References

[1] Anitha Vijayalakshmi., 2021. ERPO-OFDM for data transmission and brightness control in visible light communication system. *Optical and Quantum Electronics.*, *53*(9). doi:10.1007/s11082-021-02977-x.

[2] Park, J.S., Choi, Y.S. and Lee, W.S., 2022. Design of Miniaturized Incident Angle-Insensitive 2.45 GHz RF-Based Energy Harvesting System for IoT Applications. *IEEE Transactions on Antennas and Propagation*, *70*(5), pp. 3781–3788. doi:10.1109/TAP.2021.3137481.

[3] Saadat, W., Member, S., Raurale, S.A., Conway, G.A., Mcallister, J. and Member, S., 2022. Wearable Antennas for Human Identification at. *IEEE Transactions on Antennas and Propagation*, *70*(1), pp. 17–26.

[4] Dr. V.Prakasam, R.Meghana, A.Sravani, SK.Karishma, and B.Divya, N.C., 2021. Tumor Detection in Skin Using Electromagnetic Band Gap Stucture Antenna. *International*

Research Journal of Engineering and Technology, *08*(08), pp. 1552–1556.

[5] Indran Suyambulingam, S.M.R. and S.S., 2023. Advanced Materials and Technologies for Engineering Applications. *Applied Science and Engineering Progress*, *16*(3). doi:10.14416/j.asep.2023.01.008.

[6] Phiri, R., Rangappa, S.M., Siengchin, S. and Marinkovic, D., 2023. Agro-Waste Natural Fiber Sample Preparation Techniques for Bio-Composites Development: Methodological Insights. *Facta Universitatis, Series: Mechanical Engineering*, *21*(4), pp. 631–656. doi:10.22190/FUME230905046P.

[7] Sathish Kumar Palaniappan, Manoj Kumar Singh, S.M.R. and S.S., 2024. Eco-friendly Biocomposites: A Step Towards Achieving Sustainable Development Goals. *Applied Science and Engineering Progress*, *17*(4). doi:10.14416/j.asep.2024.02.003.

[8] Chaurasia, A.S., Shankhwar, A.K., and Singh, A., 2024. Design and analysis of the Flexible Antenna behavior for Microwave Imaging of breast cancer. *Journal of Integrated Science and Technology*, *12*(2), pp. 1–6.

[9] Oritsetimeyin, P., 2024. Design Of 2 . 4 GHZ Single Band Inset-Fed Rectangular Microstrip Patch Antenna, (January).

[10] Miranda, I., Souza, A., Sousa, P., Ribeiro, J., Castanheira, E.M.S., Lima, R. and Minas, G., 2022. Properties and applications of PDMS for biomedical engineering: A review. *Journal of Functional Biomaterials*, *13*(1). doi:10.3390/jfb13010002.

[11] Abi T Zerith M, N.M., 2020. A Compact Wearable 2 . 45 GHz Antenna for WBAN Applications. *International Conference on Devices, Circuits and Systems (ICDCS)*, pp. 184–187. doi:10.1109/ICDCS48716.2020.243577.

[12] S. Nivetha, G.A. and Preethi, C.C., 2019. Performance Evaluation of Modulation Techniques in Li-Fi. *International Journal of Recent Technology and Engineering (IJRTE)*, *8*(3).

[13] Irina Stefan, HanyElgala, H.H., 2012. Study of Dimming and LED Nonlinearity for ACO-OFDM Based VLC Systems. *IEEE Wireless Communications and Networking Conference*.

[14] Mohammed S. A. and Mossaad, S.H. (n.d.). Practical OFDM Signalling for Visible Light Communications Using Spatial Summation. *27th Biennial Symposium on Communications (QBSC)Kingston, ON, Canada*.

[15] Armstrong, J. and Lowery, A.J., 2006. Power efficient optical OFDM. *Electronics Letters*, *42*, pp. 370–372.

[16] Hasan Farahneh and Fatima Hussain, X.F., 2018. Performance analysis of adaptive OFDM modulation scheme in VLC vehicular communication network in realistic noise environment. *EURASIP Journal on Wireless Communications and Networking*.

[17] PrateekGawande, Aditya Sharma, P.K. (n.d.). Various Modulation Techniques for Li-Fi. *International Journal of Advanced Research in Computer and Communication Engineering*, *5*(3).

[18] Panda, S., Gupta, A. and Acharya, B., 2020. Wearable microstrip patch antennas with different flexible substrates for health monitoring system. *Materials Today: Proceedings*, *45*. doi:10.1016/j.matpr.2020.09.127.

[19] Bayero, G.M., Kah Wye, H. and Sree, S., 2021. Design of Antenna Array for Breast Tumor Detection. *International Journal of Infrastructure Research and Management*, *9*(2), pp. 94–103. Retrieved from https://iukl.edu.my/rmc/publications/ijirm/

[20] Mussa Elsaadi, R.H., 2023. Breast Cancer Detection Based on Multi-Slotted Patch Antenna at ISM Band. *Circuits and Systems*, *14*(5). doi:10.4236/cs.2023.145001.

[21] Yadav, Manojkumar Brijlal, Bharti Singh, V., 2017. Design of Rectangular Microstrip Patch Antenna with. *International Conference on Electronics, Communication and Aerospace Technology*, pp. 367–370.

[22] Dixit, A., Pinto, M.S. and Engineering, C., 2019. Simulation of microstrip patch antenna for detection of abnormal tissues in thyroid gland. *International Journal of Innovations in Engineering and Technology*, *13*(3), pp. 50–55.

[23] Sugumaran, B., Balasubramanian, R. and Palaniswamy, S.K., 2021. Reduced specific absorption rate compact flexible monopole antenna system for smart wearable wireless communications. *Engineering Science and Technology, an International Journal*, *24*(3), pp. 682–693. doi:10.1016/j.jestch.2020.12.012.

[24] Sinha, S., Hasan, R.R., Niloy, T.R., and Rahman, A., 2021. Antenna design and fabrication for biotelemetry applications. *International Journal of Electrical and*

Computer Engineering, *11*(4), pp. 3639–3646. doi:10.11591/ijece.v11i4.pp3639-3646.

[25] Doondi Kumar Janapala and Moses Nesasudha., 2019. Specific absorption rate reduction using metasurface unit cell for flexible polydimethylsiloxane antenna for 2 . 4 GHz wearable applications, (December 2018), pp. 1–12. doi:10.1002/mmce.21835.

[26] Sreemathy, R., Hake, S., Sulakhe, S. and Behera, S., 2020. Slit Loaded Textile Microstrip Antennas. *IETE Journal of Research*, pp. 1–9. doi:10.1080/03772063.2019.1709572.

[27] Çalışkan, R., Gültekin, S.S., Uzer, D. and Dündar, Ö., 2015. A Microstrip Patch Antenna Design for Breast Cancer Detection. *Procedia - Social and Behavioral Sciences*, *195*, pp. 2905–2911. doi:10.1016/j.sbspro.2015.06.418.

[28] Morris, S., Chandran, A.R., Timmons, N. and Morrison, J., 2016. Design and performance of a flexible and conformal PDMS Dipole antenna for WBAN applications. *European Microwave Week 2016: "Microwaves Everywhere", EuMW 2016 - Conference Proceedings; 46th European Microwave Conference, EuMC 2016*, pp. 84–87. doi:10.1109/EuMC.2016.7824283.

[29] Fu, Y., Lei, J., Zou, X. and Guo, J., 2019. Flexible antenna design on PDMS substrate for implantable bioelectronics applications. *Electrophoresis*, *40*(8), pp. 1186–1194. doi:10.1002/elps.201800497.

[30] Samal, P.B., Chen, S.J. and Fumeaux, C.,2023. Wearable Textile Multiband Antenna for WBAN Applications. *IEEE Transactions on Antennas and Propagation*, *71*(2), pp. 1391–1402. doi:10.1109/TAP.2022.3230550.

[31] Alsharif, F. and Kurnaz, C., 2018. Wearable Microstrip Patch Ultra Wide Band Antenna for Breast Cancer Detection. *2018 41st International Conference on Telecommunications and Signal Processing, TSP 2018*, pp. 456–459. doi:10.1109/TSP.2018.8441335.

[32] Hu, B., Gao, G.P., He, L. Le, Cong, X.D. and Zhao, J.N., 2016. Bending and On-Arm Effects on a Wearable Antenna for 2.45 GHz Body Area Network. *IEEE Antennas and Wireless Propagation Letters*, *15*, pp. 378–381. doi:10.1109/LAWP.2015.2446512.

[33] Sanusi, O.M., Ghaffar, F.A., Shamim, A., Vaseem, M., Wang, Y. and Roy, L., 2019. Development of a 2.45 GHz antenna for flexible compact radiation dosimeter tags. *IEEE Transactions on Antennas and Propagation*, *67*(8), pp. 5063–5072. doi:10.1109/TAP.2019.2911647.

[34] Lim, S. and Yoon, Y.J., 2021. Wideband-narrowband switchable tapered slot antenna for breast cancer diagnosis and treatment. *Applied Sciences (Switzerland)*, *11*(8). doi:10.3390/app11083606.